Physics Letters B 797 (2019) 134789

Contents lists available at ScienceDirect

Physics Letters B

www.elsevier.com/locate/physletb

Measurement of the *CP*-violating phase ϕ_s from $B_s^0 \to J/\psi\,\pi^+\pi^-$ decays in 13 TeV pp collisions

LHCb Collaboration

ARTICLE INFO

Article history:
Received 26 April 2019
Received in revised form 15 July 2019
Accepted 15 July 2019
Available online 18 July 2019
Editor: M. Doser

ABSTRACT

Decays of B_s^0 and $\overline{B}{}_s^0$ mesons into $J/\psi\,\pi^+\pi^-$ final states are studied in a data sample corresponding to 1.9 fb^{-1} of integrated luminosity collected with the LHCb detector in 13 TeV pp collisions. A time-dependent amplitude analysis is used to determine the final-state resonance contributions, the *CP*-violating phase $\phi_s = -0.057 \pm 0.060 \pm 0.011$ rad, the decay-width difference between the heavier mass B_s^0 eigenstate and the B^0 meson of $-0.050 \pm 0.004 \pm 0.004$ ps^{-1}, and the *CP*-violating parameter $|\lambda| = 1.01^{+0.08}_{-0.06} \pm 0.03$, where the first uncertainty is statistical and the second systematic. These results are combined with previous LHCb measurements in the same decay channel using 7 TeV and 8 TeV pp collisions obtaining $\phi_s = 0.002 \pm 0.044 \pm 0.012$ rad, and $|\lambda| = 0.949 \pm 0.036 \pm 0.019$.

1. Introduction

Measurements of *CP* violation in final states that can be populated both by direct decay and via mixing provide an excellent way of looking for physics beyond the Standard Model (SM) [1]. As yet unobserved heavy bosons, light bosons with extremely small couplings, or fermions can be present virtually in quantum loops, and thus affect the relative *CP* phase. Direct decays into non-flavour-specific final states can interfere with those that undergo $B_s^0 - \overline{B}{}_s^0$ mixing prior to decay. This interference can result in *CP* violation. In certain B_s^0 decays one *CP*-violating phase that can be measured, called ϕ_s, can be expressed in terms of Cabibbo–Kobayashi–Maskawa matrix elements as $-2\arg\left[-V_{ts}V_{tb}^*/V_{cs}V_{cb}^*\right]$. It is not predicted in the SM, but can be inferred with high precision from other experimental data giving a value of $-36.5^{+1.3}_{-1.2}$ mrad [2]. This number is consistent with previous measurements, which did not have enough sensitivity to determine a non-zero value [3–7]. In this paper we present the results of a new analysis of the $B_s^0 \to J/\psi\,\pi^+\pi^-$ decay using data from 13 TeV pp collisions collected using the LHCb detector in 2015 and 2016.[1] The existence of this decay and its use in *CP*-violation studies was suggested in Ref. [8].

2. Detector and simulation

The LHCb detector [9,10] is a single-arm forward spectrometer covering the pseudorapidity range $2 < \eta < 5$, designed for the study of particles containing b or c quarks. The detector includes a high-precision tracking system consisting of a silicon-strip vertex detector surrounding the pp interaction region [11], a large-area silicon-strip detector located upstream of a dipole magnet with a bending power of about 4 Tm, and three stations of silicon-strip detectors and straw drift tubes placed downstream of the magnet. The tracking system provides a measurement of the momentum, p, of charged particles with a relative uncertainty that varies from 0.5% at low momentum to 1.0% at 200 GeV.[2] The minimum distance of a track to a primary vertex (PV), the impact parameter (IP), is measured with a resolution of $(15 + 29/p_{\rm T})\,\mu$m, where $p_{\rm T}$ is the component of the momentum transverse to the beam, in GeV. Different types of charged hadrons are distinguished using information from two ring-imaging Cherenkov detectors [12]. Photons, electrons and hadrons are identified by a calorimeter system consisting of scintillating-pad and preshower detectors, an electromagnetic and a hadronic calorimeter. Muons are identified by a system composed of alternating layers of iron and multiwire proportional chambers [13]. The online event selection is performed by a trigger, which consists of a hardware stage, based on information from the calorimeter and muon systems, followed by a software stage, which applies a full event reconstruction.

At the hardware trigger stage, events are required to have a muon with high $p_{\rm T}$ or a hadron, photon or electron with high transverse energy in the calorimeters. The software trigger is composed of two stages, the first of which performs a partial reconstruction and requires either a pair of well-reconstructed, oppo-

[1] In this paper mention of a particular final state implies use of the charge-conjugate state, except when dealing with *CP*-violating processes.

[2] We use natural units where $\hbar = c = 1$.

https://doi.org/10.1016/j.physletb.2019.07.036

sitely charged muons having an invariant mass above 2.7 GeV, or a single well-reconstructed muon with $p_T > 1$ GeV and have a large IP significance $\chi^2_{IP} > 7.4$. The latter is defined as the difference in the χ^2 of the vertex fit for a given PV reconstructed with and without the considered particles. The second stage applies a full event reconstruction and for this analysis requires two opposite-sign muons to form a good-quality vertex that is well-separated from all of the PVs, and to have an invariant mass within ± 120 MeV of the known J/ψ mass [14].

Simulation is required to model the effects of the detector acceptance and the imposed selection requirements. In the simulation, pp collisions are generated using Pythia [15] with a specific LHCb configuration [16]. Decays of unstable particles are described by EvtGen [17], in which final-state radiation is generated using Photos [18]. The interaction of the generated particles with the detector, and its response, are implemented using the Geant4 toolkit [19] as described in Ref. [20].

3. Decay amplitude

The resonance structure in B^0_s and $\overline{B}{}^0_s \to J/\psi\,\pi^+\pi^-$ decays has been previously studied with a time-integrated amplitude analysis using 7 and 8 TeV pp collisions [21]. The final state was found to be compatible with being entirely CP-odd, with the CP-even state fraction below 2.3% at 95% confidence level, which allows the determination of the decay width of the heavy B^0_s mass eigenstate, Γ_H. The possible presence of a CP-even component is taken into account when determining ϕ_s [22].

The total decay amplitude for a $\overline{(}B^0_s\overline{)}$ meson at decay time equal to zero is assumed to be the sum over individual $\pi^+\pi^-$ resonant transversity amplitudes [23], and one nonresonant amplitude, with each transversity component labelled as A_i ($\overline{A}_i$). Because of the spin-1 J/ψ meson in the final state, the three possible polarizations of the J/ψ generate longitudinal (0), parallel ($\parallel$) and perpendicular ($\perp$) transversity amplitudes. When the $\pi^+\pi^-$ pair forms a spin-0 state the final system only has a longitudinal component, and thus is a pure CP eigenstate. The parameter $\lambda_i \equiv \frac{q}{p}\frac{\overline{A}_i}{A_i}$, relates CP violation in the interference between mixing and decay associated with the polarization state i for each resonance in the final state. Here the quantities q and p relate the mass and flavour eigenstates, $p \equiv \langle B^0_s|B_L\rangle$, and $q \equiv \langle \overline{B}{}^0_s|B_L\rangle$, where $|B_L\rangle$ is the lighter mass eigenstate [1]. The total amplitudes $\mathcal{A}$ and $\overline{\mathcal{A}}$ can be expressed as the sums of the individual $\overline{(}B^0_s\overline{)}$ amplitudes, $\mathcal{A} = \sum A_i$ and $\overline{\mathcal{A}} = \sum \frac{q}{p}\overline{A}_i = \sum \lambda_i A_i = \sum \eta_i |\lambda_i| e^{-i\phi_s^i} A_i$, with η_i being the CP eigenvalue of the state. For each transversity state i there is a CP-violating phase $\phi_s^i \equiv -\arg(\eta_i\lambda_i)$ [24]. Assuming that CP violation in the decay is the same for all amplitudes, then $\lambda \equiv \eta_i\lambda_i$ and $\phi_s \equiv -\arg(\lambda)$. Using $|p/q| = 1$, the decay rates for B^0_s and $\overline{B}{}^0_s$ into the $J/\psi\,\pi^+\pi^-$ final state are[3]

$$\overline{(}\Gamma\overline{)}(t) \propto e^{-\Gamma_s t}\left\{\frac{|\mathcal{A}|^2+|\overline{\mathcal{A}}|^2}{2}\cosh\frac{\Delta\Gamma_s t}{2} \pm \frac{|\mathcal{A}|^2-|\overline{\mathcal{A}}|^2}{2}\cos(\Delta m_s t) - \mathcal{R}e(\mathcal{A}^*\overline{\mathcal{A}})\sinh\frac{\Delta\Gamma_s t}{2} \mp \mathcal{I}m(\mathcal{A}^*\overline{\mathcal{A}})\sin(\Delta m_s t)\right\}, \quad (1)$$

where the $-$ sign before the $\cos(\Delta m_s t)$ term and $+$ sign before the $\sin(\Delta m_s t)$ term apply to $\overline{\Gamma}(t)$, $\Delta\Gamma_s \equiv \Gamma_L - \Gamma_H$ is the decay-width difference between the light and the heavy mass eigenstates, $\Delta m_s \equiv m_H - m_L$ is the corresponding mass difference, and $\Gamma_s \equiv (\Gamma_L + \Gamma_H)/2$ is the average B^0_s meson decay width [26].

For J/ψ decays to $\mu^+\mu^-$ final states the A_i amplitudes are themselves functions of four variables: the $\pi^+\pi^-$ invariant mass $m_{\pi\pi}$, and three angular variables $\Omega \equiv (\cos\theta_{\pi\pi}, \cos\theta_{J/\psi}, \chi)$, defined in the helicity basis. These angles are defined as $\theta_{\pi\pi}$ between the π^+ direction in the $\pi^+\pi^-$ rest frame with respect to the $\pi^+\pi^-$ direction in the B^0_s rest frame, $\theta_{J/\psi}$ between the μ^+ direction in the J/ψ rest frame with respect to the J/ψ direction in the B^0_s rest frame, and χ between the J/ψ and $\pi^+\pi^-$ decay planes in the B^0_s rest frame [22,24]. (These definitions are the same for B^0_s and $\overline{B}{}^0_s$, namely, using μ^+ and π^+ to define the angles for both B^0_s and $\overline{B}{}^0_s$ decays.) The explicit forms of the $|\mathcal{A}(m_{\pi\pi},\Omega)|^2$, $|\overline{\mathcal{A}}(m_{\pi\pi},\Omega)|^2$, and $\mathcal{A}^*(m_{\pi\pi},\Omega)\overline{\mathcal{A}}(m_{\pi\pi},\Omega)$ terms in Eq. (1) are given in Ref. [22].

The analysis proceeds by performing an unbinned maximum-likelihood fit to the $\pi^+\pi^-$ mass distribution, the decay time, and helicity angles of B^0_s candidates identified as B^0_s or $\overline{B}{}^0_s$ by a flavour-tagging algorithm [27].[4] The fit provides the CP-even and CP-odd components, and since we include the initial flavour tag, the fit also determines the CP-violating parameters ϕ_s and $|\lambda|$, and the decay width. In order to proceed, we need to select a clean sample of B^0_s decays, determine acceptance corrections, perform a calibration of the decay-time resolution in each event as a function of its uncertainty, and calibrate the flavour-tagging algorithm.

4. Selection requirements

The selection of $J/\psi\,\pi^+\pi^-$ right-sign (RS), and wrong-sign (WS) $J/\psi\,\pi^\pm\pi^\pm$ final states, proceeds in two phases. Initially we impose loose requirements and subsequently use a multivariate analysis to further suppress the combinatorial background. In the first phase we require that the J/ψ decay tracks be identified as muons, have $p_T > 500$ MeV, and form a good vertex with vertex fit χ^2 less than 16. The identified pions are required to have $p_T > 250$ MeV, not originate from any PV, and form a good vertex with the muons. The resulting B^0_s candidate is assigned to the PV for which it has the smallest χ^2_{IP}. Furthermore, we require that the smallest χ^2_{IP} is not greater than 25. The B^0_s candidate is required to have its momentum vector aligned with the vector connecting the PV to the B^0_s decay vertex, and to have a decay time greater than 0.3 ps. Reconstructed tracks sharing the same hits are vetoed.

In addition, background from $B^+ \to J/\psi\,K^+$ decays,[5] where the K^+ is misidentified as a π^+ and combined with a random π^-, is vetoed by assuming that each detected pion is a kaon, computing the $J/\psi\,K^+$ mass, and removing those candidates that are within ± 36 MeV of the known B^+ mass [14]. Backgrounds from $B^0 \to J/\psi\,K^+\pi^-$ or $B^0_s \to J/\psi\,K^+K^-$ decays with misidentified kaons result in masses lower than the B^0_s peak and thus do not need to be vetoed.

For the multivariate part of the selection, we use a Boosted Decision Tree, BDT [28,29], with the uBoost algorithm [30]. The algorithm is optimized to not further bias acceptance on the variable $\cos\theta_{\pi\pi}$. The variables used to train the BDT are the difference between the muon and pion identifications for the muon identified with lower quality, the p_T of the B^0_s candidate, the sum of the p_T of the two pions, and the natural logarithms of: the χ^2_{IP} of each of the pions, the χ^2 of the B^0_s vertex and decay tree fits [31], and the χ^2_{IP} of the B^0_s candidate. In the fit, the B^0_s momentum vector is constrained to point to the PV, the two muons are constrained to

[3] The latest LHCb measurement determined $|p/q|^2 = 1.0039 \pm 0.0033$ [25].

[4] We utilize the same likelihood construction that we used to determine ϕ_s and $|\lambda|$ in $B^0_s \to J/\psi\,K^+K^-$ decays with K^+K^- above the $\phi(1020)$ mass region [6].

[5] When discussing flavour-specific decays, mention of a particular mode implies the additional use of the charge-conjugate mode.

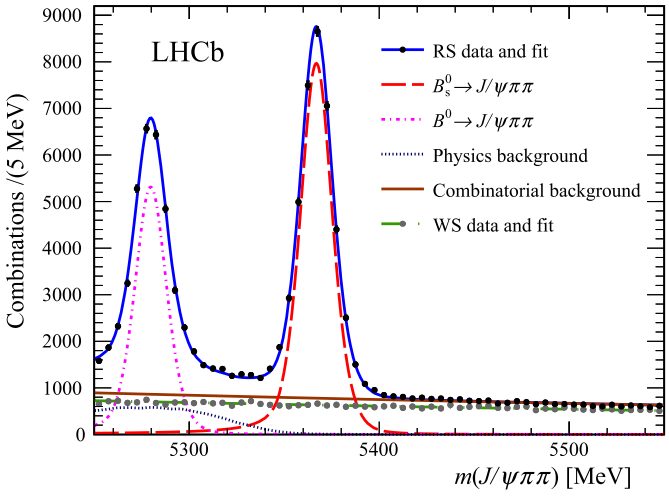

Fig. 1. Results of the simultaneous fit to the $J/\psi\,\pi\pi$ mass distributions RS (black points) and WS (grey points) samples. The solid (blue) curve shows the fit to the RS sample, the long dashed (red) curve shows the signal, the dot-dashed (magenta) curve shows $B^0 \to J/\psi\,\pi^+\pi^-$ decays, the dot-long-dashed (brown) curve shows the combinatorial background, the dotted (black) curve shows the sum of $B_s^0 \to J/\psi\,\eta'$ and Λ_b^0 background, while the dot-dot-dashed (green) curve shows the fit to WS sample.

the J/ψ mass, and all four tracks are constrained to originate from the same vertex.

Implementing uBoost requires a training procedure. Data background in the $J/\psi\,\pi^+\pi^-$ mass interval between 200 to 250 MeV above the B_s^0 mass and simulated signal are first used. Then, separate samples are used to test the BDT performance. We weight the training simulation samples to match the two-dimensional B_s^0 p and $p_{\rm T}$ distributions, and smear the vertex fit χ^2, to match the background-subtracted preselected data. Finally, the minimum requirement for BDT point is chosen to maximize signal significance, $S/\sqrt{S+B}$, where $S(B)$ is the expected signal (background) yields in a range corresponding to ± 2.5 times the mass resolution around the known B_s^0 mass [14].

To determine the signal and background yields we fit the candidate B_s^0 mass distribution. Backgrounds include combinatorics, whose shape is estimated using WS $J/\psi\,\pi^\pm\pi^\pm$ candidates modelled by an exponential function, $B_s^0 \to J/\psi\,\eta'(\to \rho^0\gamma)$ decays with the γ ignored, and $\Lambda_b^0 \to J/\psi\,pK^-$ decays with both hadrons misidentified as pions. The latter backgrounds are modelled using simulation. The B_s^0 signal shape is parameterized by a Hypatia function [32], where the signal radiative tail parameters are fixed to values obtained from simulation. The same shape parameters are used for the $B^0 \to J/\psi\,\pi^+\pi^-$ decays, with the mean value shifted by the known B_s^0 and B^0 meson mass difference [14]. Finally, we fit simultaneously both RS and WS candidates, using the simulated shape for $B_s^0 \to J/\psi\,\eta'(\to \rho^0\gamma)$ whose yield is allowed to float, and fixing both the size and shape of the $\Lambda_b^0 \to J/\psi\,pK^-$ component. The results of the fit are shown in Fig. 1. We find $33\,530 \pm 220$ signal B_s^0 within ± 20 MeV of the B_s^0 mass peak, with a purity of 84%. These decays are used for further analysis. Multiple candidates in the same event have a rate of 0.20% in a ± 20 MeV interval around the B_s^0 mass peak, and are retained.

To subtract the background in the signal region in the amplitude fit we add negatively weighted events from the WS sample to the RS sample, also accounting for the differing $\pi\pi$ mass and decay-time distributions. The weights are determined by comparing the RS and WS mass distributions in the upper mass sideband $(5420 - 5550\,\text{MeV})$. In addition, a small component of $B_s^0 \to J/\psi\,\eta'(\eta' \to \rho^0\gamma)$ decays is also subtracted, since it is absent in the WS sample.

5. Detector efficiency and resolution

The correlated efficiencies in $m_{\pi\pi}$ and angular variables Ω are determined from simulation. We weight the simulated signal events to reproduce the B_s^0 meson $p_{\rm T}$ and η distributions as well as the track multiplicity of the events. The latter may influence the efficiencies of the tracking and particle identification. The calculated efficiencies are shown in Fig. 2 along with the determined efficiency function. The four-dimensional efficiency is parameterized by a combination of Legendre and spherical harmonic moments [33], as

$$\varepsilon(m_{\pi\pi}, \cos\theta_{\pi\pi}, \cos\theta_{J/\psi}, \chi) = \sum_{a,b,c,d} \epsilon^{abcd} P_a(\cos\theta_{\pi\pi}) Y_{bc}(\theta_{J/\psi}, \chi) P_d\left(2\frac{m_{\pi\pi} - m_{\pi\pi}^{\rm min}}{m_{\pi\pi}^{\rm max} - m_{\pi\pi}^{\rm min}} - 1\right), \quad (2)$$

where P_a and P_d are Legendre polynomials, Y_{bc} are spherical harmonics, $m_{\pi\pi}^{\rm min} = 2m_{\pi^+}$ and $m_{\pi\pi}^{\rm max} = m_{B_s^0} - m_{J/\psi}$, and ϵ^{abcd} are efficiency coefficients determined from weighted averages of decays generated uniformly over phase space [6].

The model gives an excellent representation of the simulated data. The efficiency is uniform within about $\pm 4\%$ for $\cos\theta_{J/\psi}$ and about 10% for χ variables; however the $m_{\pi\pi}$ and $\cos\theta_{\pi\pi}$ variables show large efficiency variations and correlations (see Fig. 3), due to the $\chi^2_{\rm IP} > 4$ requirements on the hadrons. The loss of efficiency in the lower $m_{\pi\pi}$ region can be interpreted as the projection of the effects of cuts on $\chi^2_{\rm IP}$. Events at $\cos\theta_{\pi\pi} = \pm 1$ and $m_{\pi\pi} \simeq 0.6 - 0.8$ GeV are at the kinematic boundary of $m^2_{J/\psi\,\pi^+}$. One of the pions is almost at rest in B_s^0 rest frame, and thus the pion points to the PV, resulting in a very small $\chi^2_{\rm IP}$ for this pion. The $\chi^2_{\rm IP}$ variable is the most useful tool to suppress large pion combinatorial background from the PV.

The reconstruction efficiency is not constant as a function of B_s^0 decay time due to displacement requirements applied to the hadrons in the offline selections and on J/ψ candidates in the trigger. It is determined using the control channel $B^0 \to J/\psi\,K^*(892)^0$, with $K^*(892)^0 \to K^+\pi^-$, which is known to have a lifetime of $\tau_{B^0} = 1.520 \pm 0.004$ ps [14]. The simulated B^0 events are weighted to reproduce the distributions in the data for $p_{\rm T}$ and η of the B^0 meson, and the invariant mass and helicity angle of $K^+\pi^-$ system, as well as the track multiplicity of the events. The signal efficiency is calculated as $\varepsilon^{B_s^0}_{\rm data}(t) = \varepsilon^{B^0}_{\rm data}(t) \cdot \varepsilon^{B_s^0}_{\rm sim}(t)/\varepsilon^{B^0}_{\rm sim}(t)$, where $\varepsilon^{B^0}_{\rm data}(t)$ is the efficiency of the control channel as measured by comparing data with the known lifetime distribution, and $\varepsilon^{B_s^0}_{\rm sim}(t)/\varepsilon^{B^0}_{\rm sim}(t)$ is the ratio of efficiencies of the simulated signal and control mode after the full trigger and selection chain have been applied. This correction accounts for the small differences in the kinematics between the signal and control modes. The details of the method are explained in Ref. [4].

The acceptance is checked by measuring the decay width of $B^+ \to J/\psi\,K^+$ decays. The fitted decay-width difference between the B^+ and B^0 mesons is $\Gamma_{B^+} - \Gamma_{B^0} = -0.0475 \pm 0.0013\,\text{ps}^{-1}$, where the uncertainty is statistical only, in agreement with the known value of $-0.0474 \pm 0.0023\,\text{ps}^{-1}$ [14].

From the measured B_s^0 candidate momentum and decay distance, the decay time and its event-by-event uncertainty δ_t are calculated. The calculated uncertainty is imbedded into the resolution function, which is modelled by the sum of three Gaussian functions with common means and widths proportional to a quadratic function of δ_t. The parameters of the resolution function are determined with a sample of putative prompt $J/\psi \to \mu^+\mu^-$

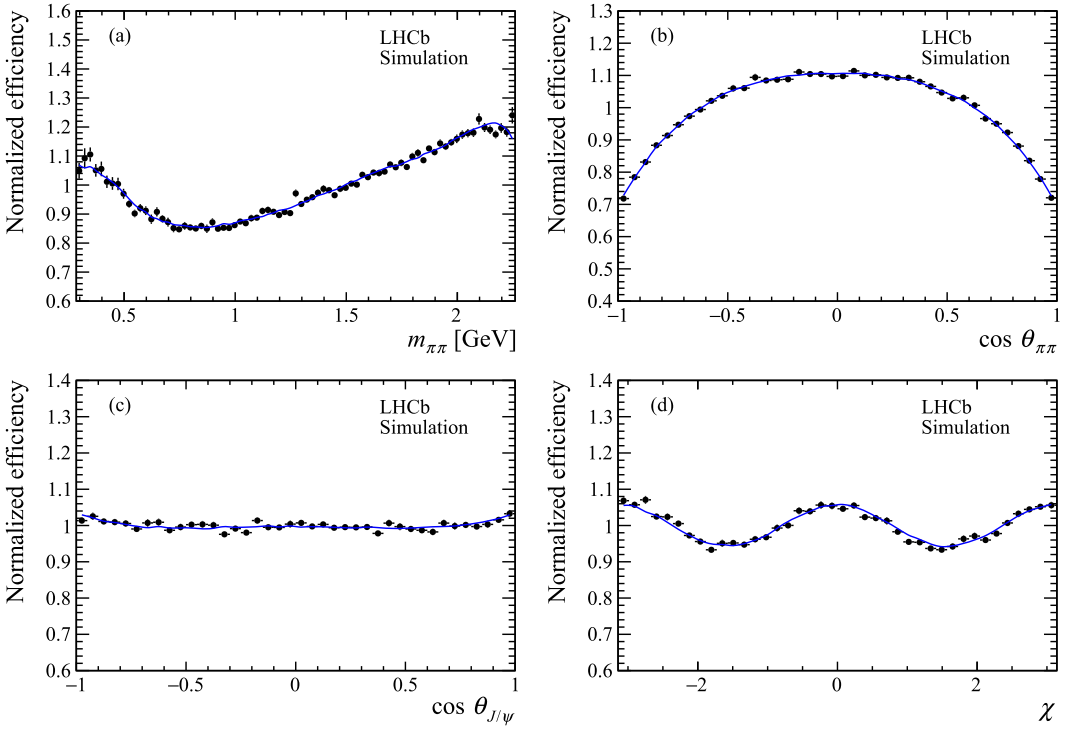

Fig. 2. Overall efficiency normalized to unity for (a) $m_{\pi\pi}$, (b) $\cos\theta_{\pi\pi}$, (c) $\cos\theta_{J\psi}$ and (d) χ observables. The points with error bars are from the $B_s^0 \to J/\psi\,\pi^+\pi^-$ simulation, while the curves show the projection of the efficiency function.

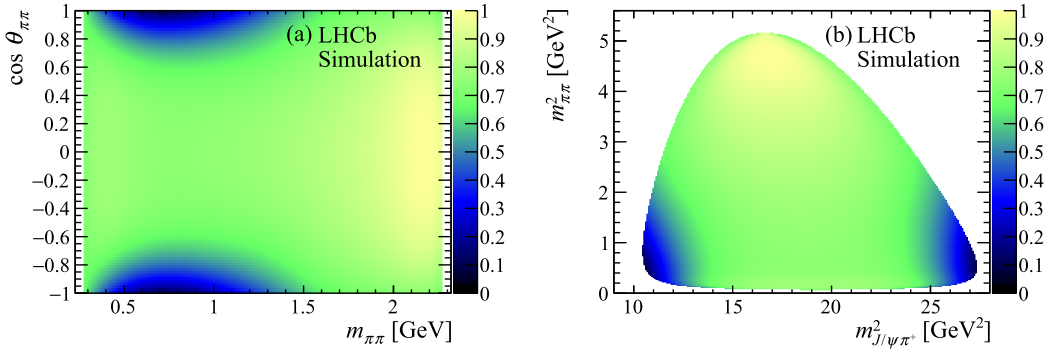

Fig. 3. Overall efficiency for (a) $m_{\pi\pi}$ vs $\cos\theta_{\pi\pi}$ and (b) $m^2_{J\psi\,\pi^+}$ vs $m^2_{\pi\pi}$. The inefficiency is at the kinematic boundary of $m^2_{J\psi\,\pi^+}$ where the pion is almost at rest in the B_s^0 frame.

decays combined with two pions of opposite charge. Taking into account the decay-time uncertainty distribution of the B_s^0 signal, the average effective resolution is found to be 41.5 fs. The method is validated using simulation; we estimate the accuracy of the resolution determination to be ±3%.

6. Flavour tagging

Knowledge of the $\overset{(-)}{B}{}^0_s$ flavour at production is necessary. We use information from decays of the other b hadron in the event (opposite-side, OS) and fragments of the jet that produced the $\overset{(-)}{B}{}^0_s$ meson that contain a charged kaon, called same-side kaon (SSK) [27]. The OS tagger infers the flavour of the other b hadron in the event from the charges of muons, electrons, kaons, and the net charge of the particles that form reconstructed secondary vertices.

The flavour tag, q, takes values of $+1$, -1 or 0 if the signal meson is tagged as B_s^0, $\overline{B}{}_s^0$ or untagged, respectively. The wrong-tag probability, η, is estimated event-by-event based on the output of a neural network. It is subsequently calibrated with data in order to relate it to the true wrong-tag probability of the event by a linear relation as

$$\begin{aligned}\omega(\eta) &= p_0 + \frac{\Delta p_0}{2} + \left(p_1 + \frac{\Delta p_1}{2}\right)\cdot(\eta - \langle\eta\rangle);\\ \overline{\omega}(\eta) &= p_0 - \frac{\Delta p_0}{2} + \left(p_1 - \frac{\Delta p_1}{2}\right)\cdot(\eta - \langle\eta\rangle),\end{aligned} \tag{3}$$

where p_0, p_1, Δp_0 and Δp_1 are calibration parameters, and $\omega(\eta)$ and $\overline{\omega}(\eta)$ are the calibrated probabilities for a wrong-tag assignment for B_s^0 and $\overline{B}{}_s^0$ mesons, respectively. The calibration is performed separately for the OS and the SSK taggers using $B^+ \to J/\psi\,K^+$ and $B_s^0 \to D_s^-\pi^+$ decays, respectively. When events are tagged by both the OS and the SSK algorithms, a combined tag decision is formed. The resulting efficiency and tagging powers are listed in Table 1.

Table 1
Tagging efficiency, $\varepsilon_{\rm tag}$, and tagging power given as the efficiency times dilution squared, $\varepsilon_{\rm tag}D^2$, where $D = (1-2\omega)$ for each category and the total. The uncertainties on $\varepsilon_{\rm tag}$ are statistical only, and those for $\varepsilon_{\rm tag}D^2$ contain both statistical and systematic components.

Category	$\varepsilon_{\rm tag}$ (%)	$\varepsilon_{\rm tag}D^2$(%)
OS only	11.0 ± 0.6	0.86 ± 0.05
SSK only	42.6 ± 0.6	1.54 ± 0.33
OS and SSK	24.9 ± 0.6	2.66 ± 0.19
Total	78.5 ± 0.7	5.06 ± 0.38

Table 2
Resonance parameters.

Resonance	Mass (MeV)	Width (MeV)	Source
$f_0(500)$	471 ± 21	534 ± 53	LHCb[38]
$f_0(980)$	Varied in fits		
$f_2(1270)$	1275.5 ± 0.8	$186.7^{+2.2}_{-2.5}$	PDG [14]
$f_0(1500)$	Varied in fits		
$f_2'(1525)$	1522.2 ± 1.7	78.0 ± 4.8	LHCb [6]
$f_0(1710)$	1723^{+6}_{-5}	139 ± 8	PDG [14]
$f_0(1790)$	1790^{+40}_{-30}	270^{+60}_{-30}	BES [37]

7. Description of the $\pi^+\pi^-$ mass spectrum

We fit the entire $\pi^+\pi^-$ mass spectrum including the resonance contributions listed in Table 2, and a nonresonant (NR) component. We use an isobar model [21]. All resonances are described by Breit–Wigner amplitudes, except for the $f_0(980)$ state, which is modelled by a Flatté function [34]. The nonresonant amplitude is treated as being constant in $m_{\pi\pi}$. Other theoretically motivated amplitude models are also proposed to describe this decay [35,36]. The previous publication [21] used an unconfirmed $f_0(1790)$ resonance, reported by the BES collaboration [37], instead of the $f_0(1710)$ state. We test which one gives a better fit.

The amplitude $A_R(m_{\pi\pi})$, generally represented by a Breit–Wigner function or a Flatté function, is used to describe the mass line shape of resonance R. To describe the resonance from the B_s^0 decays, the amplitude is combined with the B_s^0 and resonance decay properties to form the following expression

$$\mathcal{A}_R(m_{\pi\pi}) = \sqrt{2J_R+1}\sqrt{P_R P_B}F_B^{(L_B)}F_R^{(L_R)}A_R(m_{\pi\pi}) \times \left(\frac{P_B}{m_B}\right)^{L_B}\left(\frac{P_R}{m_0}\right)^{L_R}. \quad (4)$$

Here P_B is the J/ψ momentum in the B_s^0 rest frame, P_R is the momentum of either of the two hadrons in the dihadron rest frame, m_B is the B_s^0 mass, m_0 is the mass of resonance R,[6] J_R is the spin of the resonance R, L_B is the orbital angular momentum between the J/ψ meson and $\pi^+\pi^-$ system, and L_R the orbital angular momentum in the $\pi^+\pi^-$ system, and thus is the same as the spin of the $\pi^+\pi^-$ resonance. The terms $F_B^{(L_B)}$ and $F_R^{(L_R)}$ are the Blatt–Weisskopf barrier factors for the B_s^0 meson and R resonance, respectively [39]. The shape parameters for the $f_0(980)$ and $f_0(1500)$ resonances are allowed to vary.

[6] Equation (4) is modified from that used in previous publications [4,21] and follows the convention suggested by the PDG [14].

8. Likelihood definition

The decay-time distribution including flavour tagging is

$$R(\hat{t}, m_{\pi\pi}, \Omega, \mathfrak{q}|\mathfrak{y}) = \frac{1}{1+|\mathfrak{q}|}\Big[[1+\mathfrak{q}(1-2\omega(\mathfrak{y}))]\,\Gamma(\hat{t}, m_{\pi\pi}, \Omega) + [1-\mathfrak{q}(1-2\bar{\omega}(\mathfrak{y}))]\,\frac{1+A_{\rm P}}{1-A_{\rm P}}\bar{\Gamma}(\hat{t}, m_{\pi\pi}, \Omega)\Big], \quad (5)$$

where $\hat{t}$ is the true decay time, $\overset{(-)}{\Gamma}$ is defined in Eq. (1), and $A_{\rm P}$ is the production asymmetry of B_s^0 mesons.

The fit function for the signal is modified to take into account the decay-time resolution and acceptance effects resulting in

$$F(t, m_{\pi\pi}, \Omega, \mathfrak{q}|\mathfrak{y}, \delta_t) = \left[R(\hat{t}, m_{\pi\pi}, \Omega, \mathfrak{q}|\mathfrak{y}) \otimes T(t-\hat{t}|\delta_t)\right]\varepsilon_{\rm data}^{B_s^0}(t)\varepsilon(m_{\pi\pi}, \Omega), \quad (6)$$

where $\varepsilon(m_{\pi\pi}, \Omega)$ is the efficiency as a function of $m_{\pi\pi}$ and angular variables, $T(t-\hat{t}|\delta_t)$ is the decay-time resolution function, and $\varepsilon_{\rm data}^{B_s^0}(t)$ is the decay-time acceptance function. The free parameters in the fit are ϕ_s, $|\lambda|$, $\Gamma_{\rm H} - \Gamma_{B^0}$, the magnitudes and phases of the resonances amplitudes, and the shape parameters of some resonances. The other parameters, including Δm_s, and $\Gamma_{\rm L}$, are fixed to the known values [14] or other measurements mentioned below.

The signal function is normalized by summing over $\mathfrak{q}$ values and integrating over decay time t, the mass $m_{\pi\pi}$, and the angular variables, Ω, giving

$$\mathcal{N}(\delta_t) = 2\int [\Gamma(\hat{t}, m_{\pi\pi}, \Omega) + \frac{1+A_{\rm P}}{1-A_{\rm P}}\bar{\Gamma}(\hat{t}, m_{\pi\pi}, \Omega)] \otimes T(t-\hat{t}|\delta_t)\varepsilon_{\rm data}^{B_s^0}(t)\varepsilon(m_{\pi\pi}, \Omega)\,{\rm d}m_{\pi\pi}\,{\rm d}\Omega\,{\rm d}t\,. \quad (7)$$

We assume no asymmetries in the tagging efficiencies, which are accounted for in the systematic uncertainties. The resulting signal PDF is

$$\mathcal{P}(t, m_{\pi\pi}, \Omega, \mathfrak{q}|\mathfrak{y}, \delta_t) = \frac{1}{\mathcal{N}(\delta_t)}F(t, m_{\pi\pi}, \Omega, \mathfrak{q}|\mathfrak{y}, \delta_t). \quad (8)$$

The fitter uses a technique similar to *sPlot* [40] to subtract background from the log-likelihood sum. Each candidate is assigned a weight, $W_i = +1$ for the RS events and negative values for the WS events. The likelihood function is defined as

$$-2\ln\mathcal{L} = -2\,s_W\sum_i W_i \ln\mathcal{P}(t, m_{\pi\pi}, \Omega, \mathfrak{q}|\mathfrak{y}, \delta_t), \quad (9)$$

where $s_W \equiv \sum_i W_i / \sum_i W_i^2$ is a constant factor accounting for the effect of the background subtraction on the statistical uncertainty.

The decay-time acceptance is assumed to be factorized from other variables, but due to the $\chi^2_{\rm IP}$ cut on the two pions, the decay time is correlated with the angular variables. To avoid bias on the determination of $\Gamma_{\rm H}$ from the decay-time acceptance, the simulated B_s^0 signal is weighted in order to reproduce the $m_{\pi\pi}$ resonant structure observed in data by using the preferred amplitude model that is determined by the overall fit. An iterative procedure is performed to finalize the decay-time acceptance. This procedure converges in three steps beyond which $\Gamma_{\rm H}$ does not vary. When we apply this method to pseudoexperiments that include the correlation mentioned before, the fitter reproduces the input values of ϕ_s, $\Gamma_{\rm H}$ and $|\lambda|$.

Table 3
Likelihoods of various resonance model fits. Positive or negative interferences (Int) among the contributing resonances are indicated. The Solutions are indicated by #.

#	Resonance content	Int	$-2\ln\mathcal{L}$
I	$f_0(980)+f_0(1500)+f_0(1790)+f_2(1270)+f_2'(1525)$+NR	−	−4850
II	$f_0(980)+f_0(1500)+f_0(1710)+f_2(1270)+f_2'(1525)$+NR	+	−4834
III	$f_0(980)+f_0(1500)+f_0(1790)+f_2(1270)+f_2'(1525)$+NR	+	−4830
IV	$f_0(980)+f_0(1500)+f_0(1790)+f_2(1270)+f_2'(1525)$	−	−4828
V	$f_0(980)+f_0(1500)+f_0(1710)+f_2(1270)+f_2'(1525)$	−	−4706

Table 4
Fit results for the *CP*-violating parameters for Solution I. The first uncertainties are statistical, and the second systematic. The last three columns show the statistical correlation coefficients for the three parameters.

	Fit result	Correlation		
Parameter		$\Gamma_H-\Gamma_{B^0}$	$\lvert\lambda\rvert$	ϕ_s
$\Gamma_H-\Gamma_{B^0}$ (ps^{-1})	$-0.050\pm0.004\pm0.004$	1.000	0.022	0.038
$\lvert\lambda\rvert$	$1.01^{+0.08}_{-0.06}\pm0.03$	0.022	1.000	0.065
ϕ_s (rad)	$-0.057\pm0.060\pm0.011$	0.038	0.065	1.000

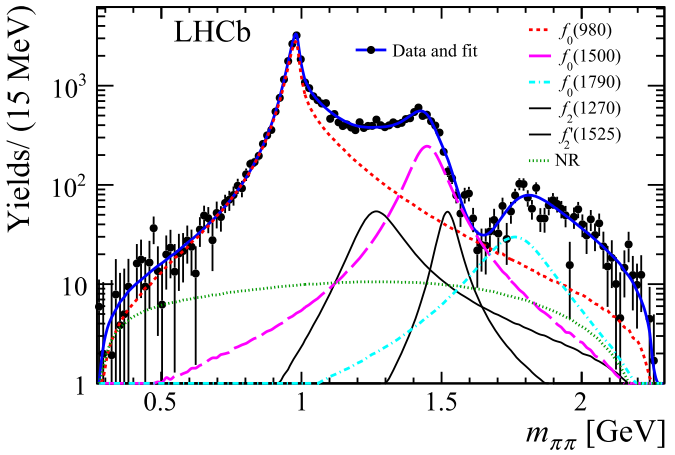

Fig. 5. Data distribution of $m_{\pi\pi}$ with the projection of the Solution I fit result overlaid. The data are described by the points (black) with error bars. The solid (blue) curve shows the overall fit.

9. Fit results

We first choose the resonances that best fit the $m_{\pi\pi}$ distribution. Table 3 lists the different fit components and the value of $-2\ln\mathcal{L}$. In these comparisons, the mass and width of most resonances are fixed to the central values listed in Table 2, except for the $f_0(980)$ and $f_0(1500)$ resonances, whose parameters are allowed to vary. We find two types of fit results, one with a positive integrated sum of all interfering components and one with a negative one. The first listed Solution I is better than Solution II by four standard deviations, calculated by taking the square root of the $-2\ln\mathcal{L}$ difference. We take Solution I for our measurement and II for systematic uncertainty evaluation. The models corresponding to Solutions I and II are very similar to those found in our previous analysis of the same final state [21].

For the fit we assume that the *CP*-violation quantities (ϕ_{si}, $|\lambda_i|$) are the same for all the resonances. We also fix Δm_s to the central value of the world average $17.757\pm0.021\,\mathrm{ps}^{-1}$ [14], and fix Γ_L to the central value of $0.6995\pm0.0047\,\mathrm{ps}^{-1}$ from the LHCb $B_s^0\to J/\psi\,K^+K^-$ results [6].

The fit values and correlations of the *CP*-violating parameters are shown in Table 4 for Solution I. The shape parameters of $f_0(980)$ and $f_0(1500)$ resonances are found to be consistent with our previous results [21]. The angular and decay-time fit projections are shown in Fig. 4. The $m_{\pi\pi}$ fit projection is shown in Fig. 5, where the contributions of the individual resonances are also displayed. All solutions listed in Table 3 give very similar fit values for ϕ_s and Γ_H. We also find that the *CP*-odd fraction is greater than 97% at 95% confidence level. The resonant content for Solutions I and II are listed in Table 5.

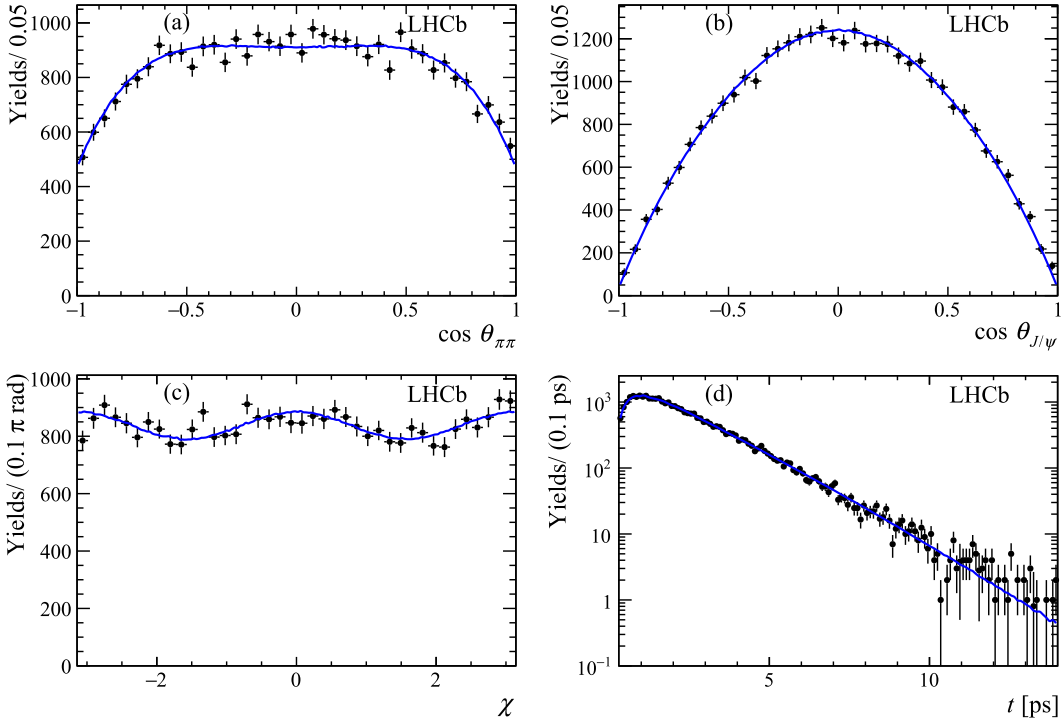

Fig. 4. Projections of the angular and decay-time variables with the fit result overlaid. The points (black) show the data and the curves (blue) the fits.

Table 5
Fit results of the resonant structure for both Solutions I and II. These results do not supersede those in Ref. [21] for the resonant fractions because no systematic uncertainties are quoted. The sum of fit fraction is not necessary 100% due to possible interferences between resonances with the same spin.

Component	Fit fractions (%)	Transversity fractions (%)		
		0	$\parallel$	$\perp$
Solution I				
$f_0(980)$	60.09 ± 1.48	100	–	–
$f_0(1500)$	8.88 ± 0.87	100	–	–
$f_0(1790)$	1.72 ± 0.29	100	–	–
$f_2(1270)$	3.24 ± 0.48	13 ± 3	37 ± 9	50 ± 10
$f_2'(1525)$	1.23 ± 0.86	40 ± 13	31 ± 14	29 ± 25
NR	2.64 ± 0.73	100	–	–
Solution II				
$f_0(980)$	93.05 ± 1.12	100	–	–
$f_0(1500)$	6.47 ± 0.41	100	–	–
$f_0(1710)$	0.74 ± 0.11	100	–	–
$f_2(1270)$	3.22 ± 0.44	17 ± 4	30 ± 8	53 ± 10
$f_2'(1525)$	1.44 ± 0.36	35 ± 8	31 ± 12	34 ± 17
NR	8.13 ± 0.79	100	–	–

10. Systematic uncertainties

The systematic uncertainties for the *CP*-violating parameters, λ and ϕ_s, are smaller than the statistical ones. They are summarized in Table 6 along with the uncertainty on $\Gamma_{\rm H} - \Gamma_{B^0}$. The uncertainty on the decay-time acceptance is found by varying the parameters of the acceptance function within their uncertainties and repeating the fit. The same procedure is followed for the uncertainties on the B^0 lifetime, Δm_s, Γ_L, $m_{\pi\pi}$ and angular efficiencies, resonance masses and widths, flavour-tagging calibration, and allowing for a 2% production asymmetry [41]; this uncertainty also includes any possible difference in flavour tagging between $\overline{B}{}^0_s$ and B^0_s. Simulation is used to validate the method for the time-resolution calibration. The uncertainties of the parameters of the time-resolution model are estimated using the difference between the signal simulation and prompt J/ψ simulation. These uncertainties are varied to obtain the effects on the physics parameters. Resonance modelling uncertainty includes varying the Breit–Wigner barrier factors, changing the default values of $L_B = 1$ for the D-wave resonances to one or two, the differences between the two best solutions, and replacing the NR component by the $f_0(500)$ resonance. Furthermore, including an isospin-violating $\rho(770)^0$ component in the fit, results in a negligible contribution of $(1.1 \pm 0.3)\%$. The largest shift among the modelling variations is taken as systematic uncertainty. The inclusion of ρ components results in the largest shifts of the three physics parameters quoted. The process $B_c^+ \to \pi^+ B^0_s$ can affect the measurement of $\Gamma_{\rm H} - \Gamma_{B^0}$. An estimate of the fraction of these decays in our sample is 0.8% [5]. Neglecting the B_c^+ contribution leads to a bias of $0.0005\,{\rm ps}^{-1}$, which is added as a systematic uncertainty. Other parameters are unchanged.

Corrections from penguin amplitudes are ignored because their effects are known to be small [42–44] compared to the current experimental precision.

11. Conclusions

Using B^0_s and $\overline{B}{}^0_s \to J/\psi\,\pi^+\pi^-$ decays, we measure the *CP*-violating phase, $\phi_s = -0.057 \pm 0.060 \pm 0.011$ rad, the decay-width difference $\Gamma_{\rm H} - \Gamma_{B^0} = -0.050 \pm 0.004 \pm 0.004\ {\rm ps}^{-1}$, and the parameter $|\lambda| = 1.01^{+0.08}_{-0.06} \pm 0.03$, where the quoted uncertainties are statistical and systematic. These results are more precise than those obtained from the previous study of this mode using 7 TeV and 8 TeV pp collisions (Run 1) [4]. To combine the Run-1 results with these, we reanalyze them by fixing $\Delta m_s = 17.757 \pm 0.021\ {\rm ps}^{-1}$ from Ref. [14], and $\Gamma_{\rm L} = 0.6995 \pm 0.0047\ {\rm ps}^{-1}$ from the LHCb $B^0_s \to J/\psi\,K^+K^-$ results [6]. We remove the Gaussian constraint on $\Delta\Gamma_s$ and let $\Gamma_{\rm H}$ vary. Instead of taking the uncertainties of flavour tagging and decay-time resolution into the statistical uncertainty, we place these sources in the systematic uncertainty and assume 100% correlation with our new results. The updated results are: $\phi_s = 0.075 \pm 0.065 \pm 0.014$ rad and $|\lambda| = 0.898 \pm 0.051 \pm 0.013$ with a correlation of 0.025. We then use the updated ϕ_s and $|\lambda|$ Run-1 results as a constraint into our new ϕ_s fit.[7] The combined results are $\Gamma_{\rm H} - \Gamma_{B^0} = -0.050 \pm 0.004 \pm 0.004\ {\rm ps}^{-1}$, $|\lambda| = 0.949 \pm 0.036 \pm 0.019$, and $\phi_s = 0.002 \pm 0.044 \pm 0.012$ rad. The correlation coefficients among the fit parameters are 0.025 (ρ_{12}), -0.001 (ρ_{13}), and 0.026 (ρ_{23}).

Our results still have uncertainties greater than the SM prediction and are slightly more precise than the measurement using $B^0_s \to J/\psi\,K^+K^-$ decays, based only on Run-1 data, which has a precision of 0.049 rad [5]. Hence this is the most precise determination of ϕ_s to date.

Table 6
Absolute systematic uncertainties for the physics parameters.

Source	$\Gamma_{\rm H} - \Gamma_{B^0}$ [$\rm fs^{-1}$]	$\lvert\lambda\rvert$ [$\times 10^{-3}$]	ϕ_s [mrad]
Decay-time acceptance	2.0	0.0	0.3
τ_{B^0}	0.2	0.5	0.0
Efficiency ($m_{\pi\pi}$, Ω)	0.2	0.1	0.0
Decay-time resolution width	0.0	4.3	4.0
Decay-time resolution mean	0.3	1.2	0.3
Background	3.0	2.7	0.6
Flavour tagging	0.0	2.2	2.3
Δm_s	0.3	4.6	2.5
$\Gamma_{\rm L}$	0.3	0.4	0.4
B_c^+	0.5	–	–
Resonance parameters	0.6	1.9	0.8
Resonance modelling	0.5	28.9	9.0
Production asymmetry	0.3	0.6	3.4
Total	3.8	29.9	11.0

Acknowledgements

We express our gratitude to our colleagues in the CERN accelerator departments for the excellent performance of the LHC. We thank the technical and administrative staff at the LHCb institutes. We acknowledge support from CERN and from the national agencies: CAPES, CNPq, FAPERJ and FINEP (Brazil); MOST and NSFC (China); CNRS/IN2P3 (France); BMBF, DFG and MPG (Germany); INFN (Italy); NWO (Netherlands); MNiSW and NCN (Poland); MEN/IFA (Romania); MSHE (Russia); MINECO (Spain); SNSF and SER (Switzerland); NASU (Ukraine); STFC (United Kingdom); NSF (USA). We acknowledge the computing resources that are provided by CERN, IN2P3 (France), KIT and DESY (Germany), INFN (Italy), SURF (Netherlands), PIC (Spain), GridPP (United Kingdom), RRCKI and Yandex LLC (Russia), CSCS (Switzerland), IFIN-HH (Romania), CBPF (Brazil), PL-GRID (Poland) and OSC (USA). We are indebted to the communities behind the multiple open-source software packages on which we depend. Individual groups or members have received support from AvH Foundation (Germany); EPLANET, Marie Skłodowska-Curie Actions and ERC (European Union); ANR, Labex P2IO and OCEVU, and Région Auvergne-

[7] We do not include an average value of $\Gamma_{\rm H}$ since no systematic uncertainty was assigned for the Run-1 result.

Rhône-Alpes (France); Key Research Program of Frontier Sciences of CAS, CAS PIFI, and the Thousand Talents Program (China); RFBR, RSF and Yandex LLC (Russia); GVA, XuntaGal and GENCAT (Spain); the Royal Society and the Leverhulme Trust (United Kingdom); Laboratory Directed Research and Development program of LANL (USA).

References

[1] I.I.Y. Bigi, A.I. Sanda, CP violation, Camb. Monogr. Part. Phys. Nucl. Phys. Cosmol. 9 (2000) 1.

[2] CKMfitter group, J. Charles, et al., Current status of the Standard Model CKM fit and constraints on $\Delta F = 2$ new physics, Phys. Rev. D 91 (2015) 073007, arXiv:1501.05013, updated results and plots available at http://ckmfitter.in2p3.fr/.

[3] CDF collaboration, T. Aaltonen, et al., First flavor-tagged determination of bounds on mixing-induced CP violation in $B_s^0 \to J/\psi\phi$ decays, Phys. Rev. Lett. 100 (2008) 161802, arXiv:0712.2397;
D0 collaboration, V.M. Abazov, et al., Measurement of B_s^0 mixing parameters from the flavor-tagged decay $B_s^0 \to J/\psi\phi$, Phys. Rev. Lett. 101 (2008) 241801, arXiv:0802.2255;
CDF collaboration, T. Aaltonen, et al., Measurement of the CP-violating phase $\beta_s^{J/\psi\phi}$ in $B_s^0 \to J/\psi\phi$ decays with the CDF II detector, Phys. Rev. D 85 (2012) 072002, arXiv:1112.1726;
D0 collaboration, V.M. Abazov, et al., Measurement of the CP-violating phase $\phi_s^{J/\psi\phi}$ using the flavor-tagged decay $B_s^0 \to J/\psi\phi$ in 8 fb^{-1} of $p\overline{p}$ collisions, Phys. Rev. D 85 (2012) 032006, arXiv:1109.3166.

[4] LHCb collaboration, R. Aaij, et al., Measurement of the CP-violating phase ϕ_s in $\overline{B}_s^0 \to J/\psi\,\pi^+\pi^-$ decays, Phys. Lett. B 736 (2014) 186, arXiv:1405.4140.

[5] LHCb collaboration, R. Aaij, et al., Precision measurement of CP violation in $B_s^0 \to J/\psi\,K^+K^-$ decays, Phys. Rev. Lett. 114 (2015) 041801, arXiv:1411.3104.

[6] LHCb collaboration, R. Aaij, et al., Resonances and CP violation in B_s^0 and $\overline{B}_s^0 \to J/\psi\,K^+K^-$ decays in the mass region above the $\phi(1020)$, J. High Energy Phys. 08 (2017) 037, arXiv:1704.08217.

[7] ATLAS collaboration, G. Aad, et al., Measurement of the CP-violating phase ϕ_s and the B_s^0 meson decay width difference with $B_s^0 \to J/\psi\phi$ decays in ATLAS, J. High Energy Phys. 08 (2016) 147, arXiv:1601.03297;
CMS collaboration, V. Khachatryan, et al., Measurement of the CP-violating weak phase ϕ_s and the decay width difference $\Delta\Gamma_s$ using the $B_s^0 \to J/\psi\,\phi(1020)$ decay channel in pp collisions at $\sqrt{s} = 8$ TeV, Phys. Lett. B 757 (2016) 97, arXiv:1507.07527.

[8] S. Stone, L. Zhang, S-waves and the measurement of CP violating phases in B_s decays, Phys. Rev. D 79 (2009) 074024, arXiv:0812.2832.

[9] LHCb collaboration, A.A. Alves Jr., et al., The LHCb detector at the LHC, J. Instrum. 3 (2008) S08005.

[10] LHCb collaboration, R. Aaij, et al., LHCb detector performance, Int. J. Mod. Phys. A 30 (2015) 1530022, arXiv:1412.6352.

[11] R. Aaij, et al., Performance of the LHCb vertex locator, J. Instrum. 9 (2014) P09007, arXiv:1405.7808.

[12] M. Adinolfi, et al., Performance of the LHCb RICH detector at the LHC, Eur. Phys. J. C 73 (2013) 2431, arXiv:1211.6759.

[13] A.A. Alves Jr., et al., Performance of the LHCb muon system, J. Instrum. 8 (2013) P02022, arXiv:1211.1346.

[14] Particle Data Group, M. Tanabashi, et al., Review of particle physics, Phys. Rev. D 98 (2018) 030001.

[15] T. Sjöstrand, S. Mrenna, P. Skands, PYTHIA 6.4 physics and manual, J. High Energy Phys. 05 (2006) 026, arXiv:hep-ph/0603175;
T. Sjöstrand, S. Mrenna, P. Skands, A brief introduction to PYTHIA 8.1, Comput. Phys. Commun. 178 (2008) 852, arXiv:0710.3820.

[16] I. Belyaev, et al., Handling of the generation of primary events in Gauss, the LHCb simulation framework, J. Phys. Conf. Ser. 331 (2011) 032047.

[17] D.J. Lange, The EvtGen particle decay simulation package, Nucl. Instrum. Methods A 462 (2001) 152.

[18] P. Golonka, Z. Was, PHOTOS Monte Carlo: a precision tool for QED corrections in Z and W decays, Eur. Phys. J. C 45 (2006) 97, arXiv:hep-ph/0506026.

[19] Geant4 collaboration, J. Allison, et al., Geant4 developments and applications, IEEE Trans. Nucl. Sci. 53 (2006) 270;
Geant4 collaboration, S. Agostinelli, et al., Geant4: a simulation toolkit, Nucl. Instrum. Methods A 506 (2003) 250.

[20] M. Clemencic, et al., The LHCb simulation application, Gauss: design, evolution and experience, J. Phys. Conf. Ser. 331 (2011) 032023.

[21] LHCb collaboration, R. Aaij, et al., Measurement of resonant and CP components in $\overline{B}_s^0 \to J/\psi\,\pi^+\pi^-$ decays, Phys. Rev. D 89 (2014) 092006, arXiv:1402.6248.

[22] L. Zhang, S. Stone, Time-dependent Dalitz-plot formalism for $B_q^0 \to J/\psi h^+h^-$, Phys. Lett. B 719 (2013) 383, arXiv:1212.6434.

[23] A.S. Dighe, I. Dunietz, H.J. Lipkin, J.L. Rosner, Angular distributions and lifetime differences in $B_s^0 \to J/\psi\phi$ decays, Phys. Lett. B 369 (1996) 144, arXiv:hep-ph/9511363.

[24] LHCb collaboration, R. Aaij, et al., Measurement of CP violation and the B_s^0 meson decay width difference with $B_s^0 \to J/\psi K^+K^-$ and $B_s^0 \to J/\psi\pi^+\pi^-$ decays, Phys. Rev. D 87 (2013) 112010, arXiv:1304.2600.

[25] LHCb collaboration, R. Aaij, et al., Measurement of the CP asymmetry in B_s^0–$\overline{B}_s^0$ mixing, Phys. Rev. Lett. 117 (2016) 061803, arXiv:1605.09768.

[26] U. Nierste, Three lectures on meson mixing and CKM phenomenology, arXiv:0904.1869.

[27] LHCb collaboration, R. Aaij, et al., Opposite-side flavour tagging of B mesons at the LHCb experiment, Eur. Phys. J. C 72 (2012) 2022, arXiv:1202.4979;
LHCb collaboration, R. Aaij, et al., A new algorithm for identifying the flavour of B_s^0 mesons at LHCb, J. Instrum. 11 (2016) P05010, arXiv:1602.07252;
D. Fazzini, Flavour tagging in the LHCb experiment, PoS LHCP2018 (2018) 230.

[28] L. Breiman, J.H. Friedman, R.A. Olshen, C.J. Stone, Classification and Regression Trees, Wadsworth International Group, Belmont, California, USA, 1984.

[29] Y. Freund, R.E. Schapire, A decision-theoretic generalization of on-line learning and an application to boosting, J. Comput. Syst. Sci. 55 (1997) 119.

[30] J. Stevens, M. Williams, uBoost: a boosting method for producing uniform selection efficiencies from multivariate classifiers, J. Instrum. 8 (2013) P12013, arXiv:1305.7248.

[31] W.D. Hulsbergen, Decay chain fitting with a Kalman filter, Nucl. Instrum. Methods A 552 (2005) 566, arXiv:physics/0503191.

[32] D. Martínez Santos, F. Dupertuis, Mass distributions marginalized over per-event errors, Nucl. Instrum. Methods A 764 (2014) 150, arXiv:1312.5000.

[33] LHCb collaboration, R. Aaij, et al., Observation of the decay $\overline{B}_s^0 \to J/\psi\,(2S)K^+\pi^-$, Phys. Lett. B 747 (2015) 484, arXiv:1503.07112.

[34] S.M. Flatté, On the nature of 0^+ mesons, Phys. Lett. B 63 (1976) 228.

[35] J. Daub, C. Hanhart, B. Kubis, A model-independent analysis of final-state interactions in $\overline{B}_{d/s}^0 \to J/\psi\pi^+\pi^-$, J. High Energy Phys. 02 (2016) 009, arXiv:1508.06841.

[36] S. Ropertz, C. Hanhart, B. Kubis, A new parametrization for the scalar pion form factors, Eur. Phys. J. C 78 (2018) 1000, arXiv:1809.06867.

[37] BES collaboration, M. Ablikim, et al., Resonances in $J/\psi \to \phi\pi^+\pi^-$ and ϕK^+K^-, Phys. Lett. B 607 (2005) 243, arXiv:hep-ex/0411001.

[38] LHCb collaboration, R. Aaij, et al., Analysis of the resonant components in $\overline{B}^0 \to J/\psi\,\pi^+\pi^-$, Phys. Rev. D 87 (2013) 052001, arXiv:1301.5347.

[39] LHCb collaboration, R. Aaij, et al., Analysis of the resonant components in $\overline{B}_s^0 \to J/\psi\pi^+\pi^-$, Phys. Rev. D 86 (2012) 052006, arXiv:1204.5643.

[40] M. Pivk, F.R. Le Diberder, sPlot: a statistical tool to unfold data distributions, Nucl. Instrum. Methods A 555 (2005) 356, arXiv:physics/0402083;
Y. Xie, sFit: a method for background subtraction in maximum likelihood fit, arXiv:0905.0724.

[41] LHCb collaboration, R. Aaij, et al., Measurement of B^0, B_s^0, B^+ and Λ_b^0 production asymmetries in 7 and 8 TeV proton-proton collisions, Phys. Lett. B 774 (2017) 139, arXiv:1703.08464.

[42] R. Fleischer, Theoretical prospects for B physics, PoS FPCP2015 (2015) 002, arXiv:1509.00601.

[43] LHCb collaboration, R. Aaij, et al., Measurement of the CP-violating phase β in $\overline{B}^0 \to J/\psi\,\pi^+\pi^-$ decays and limits on penguin effects, Phys. Lett. B 742 (2015) 38, arXiv:1411.1634.

[44] LHCb collaboration, R. Aaij, et al., Measurement of CP violation parameters and polarisation fractions in $B_s^0 \to J/\psi\,\overline{K}^{*0}$ decays, J. High Energy Phys. 11 (2015) 082, arXiv:1509.00400.

LHCb Collaboration

R. Aaij [29], C. Abellán Beteta [46], B. Adeva [43], M. Adinolfi [50], C.A. Aidala [77], Z. Ajaltouni [7], S. Akar [61], P. Albicocco [20], J. Albrecht [12], F. Alessio [44], M. Alexander [55], A. Alfonso Albero [42], G. Alkhazov [41], P. Alvarez Cartelle [57], A.A. Alves Jr [43], S. Amato [2], Y. Amhis [9], L. An [19], L. Anderlini [19], G. Andreassi [45], M. Andreotti [18], J.E. Andrews [62], F. Archilli [29], J. Arnau Romeu [8], A. Artamonov [40], M. Artuso [63], K. Arzymatov [38], E. Aslanides [8], M. Atzeni [46], B. Audurier [24], S. Bachmann [14], J.J. Back [52], S. Baker [57],

V. Balagura [9,b], W. Baldini [18,44], A. Baranov [38], R.J. Barlow [58], G.C. Barrand [9], S. Barsuk [9], W. Barter [57], M. Bartolini [21], F. Baryshnikov [73], V. Batozskaya [33], B. Batsukh [63], A. Battig [12], V. Battista [45], A. Bay [45], F. Bedeschi [26], I. Bediaga [1], A. Beiter [63], L.J. Bel [29], S. Belin [24], N. Beliy [4], V. Bellee [45], N. Belloli [22,i], K. Belous [40], I. Belyaev [35], G. Bencivenni [20], E. Ben-Haim [10], S. Benson [29], S. Beranek [11], A. Berezhnoy [36], R. Bernet [46], D. Berninghoff [14], E. Bertholet [10], A. Bertolin [25], C. Betancourt [46], F. Betti [17,e], M.O. Bettler [51], Ia. Bezshyiko [46], S. Bhasin [50], J. Bhom [31], M.S. Bieker [12], S. Bifani [49], P. Billoir [10], A. Birnkraut [12], A. Bizzeti [19,u], M. Bjørn [59], M.P. Blago [44], T. Blake [52], F. Blanc [45], S. Blusk [63], D. Bobulska [55], V. Bocci [28], O. Boente Garcia [43], T. Boettcher [60], A. Bondar [39,x], N. Bondar [41], S. Borghi [58,44], M. Borisyak [38], M. Borsato [14], M. Boubdir [11], T.J.V. Bowcock [56], C. Bozzi [18,44], S. Braun [14], M. Brodski [44], J. Brodzicka [31], A. Brossa Gonzalo [52], D. Brundu [24,44], E. Buchanan [50], A. Buonaura [46], C. Burr [58], A. Bursche [24], J. Buytaert [44], W. Byczynski [44], S. Cadeddu [24], H. Cai [67], R. Calabrese [18,g], R. Calladine [49], M. Calvi [22,i], M. Calvo Gomez [42,m], A. Camboni [42,m], P. Campana [20], D.H. Campora Perez [44], L. Capriotti [17,e], A. Carbone [17,e], G. Carboni [27], R. Cardinale [21], A. Cardini [24], P. Carniti [22,i], K. Carvalho Akiba [2], G. Casse [56], M. Cattaneo [44], G. Cavallero [21], R. Cenci [26,p], D. Chamont [9], M.G. Chapman [50], M. Charles [10,44], Ph. Charpentier [44], G. Chatzikonstantinidis [49], M. Chefdeville [6], V. Chekalina [38], C. Chen [3], S. Chen [24], S.-G. Chitic [44], V. Chobanova [43], M. Chrzaszcz [44], A. Chubykin [41], P. Ciambrone [20], X. Cid Vidal [43], G. Ciezarek [44], F. Cindolo [17], P.E.L. Clarke [54], M. Clemencic [44], H.V. Cliff [51], J. Closier [44], V. Coco [44], J.A.B. Coelho [9], J. Cogan [8], E. Cogneras [7], L. Cojocariu [34], P. Collins [44], T. Colombo [44], A. Comerma-Montells [14], A. Contu [24], G. Coombs [44], S. Coquereau [42], G. Corti [44], C.M. Costa Sobral [52], B. Couturier [44], G.A. Cowan [54], D.C. Craik [60], A. Crocombe [52], M. Cruz Torres [1], R. Currie [54], C.L. Da Silva [78], E. Dall'Occo [29], J. Dalseno [43,v], C. D'Ambrosio [44], A. Danilina [35], P. d'Argent [14], A. Davis [58], O. De Aguiar Francisco [44], K. De Bruyn [44], S. De Capua [58], M. De Cian [45], J.M. De Miranda [1], L. De Paula [2], M. De Serio [16,d], P. De Simone [20], J.A. de Vries [29], C.T. Dean [55], W. Dean [77], D. Decamp [6], L. Del Buono [10], B. Delaney [51], H.-P. Dembinski [13], M. Demmer [12], A. Dendek [32], D. Derkach [74], O. Deschamps [7], F. Desse [9], F. Dettori [24], B. Dey [68], A. Di Canto [44], P. Di Nezza [20], S. Didenko [73], H. Dijkstra [44], F. Dordei [24], M. Dorigo [44,y], A.C. dos Reis [1], A. Dosil Suárez [43], L. Douglas [55], A. Dovbnya [47], K. Dreimanis [56], L. Dufour [44], G. Dujany [10], P. Durante [44], J.M. Durham [78], D. Dutta [58], R. Dzhelyadin [40,†], M. Dziewiecki [14], A. Dziurda [31], A. Dzyuba [41], S. Easo [53], U. Egede [57], V. Egorychev [35], S. Eidelman [39,x], S. Eisenhardt [54], U. Eitschberger [12], R. Ekelhof [12], L. Eklund [55], S. Ely [63], A. Ene [34], S. Escher [11], S. Esen [29], T. Evans [61], A. Falabella [17], C. Färber [44], N. Farley [49], S. Farry [56], D. Fazzini [22,i], M. Féo [44], P. Fernandez Declara [44], A. Fernandez Prieto [43], F. Ferrari [17,e], L. Ferreira Lopes [45], F. Ferreira Rodrigues [2], S. Ferreres Sole [29], M. Ferro-Luzzi [44], S. Filippov [37], R.A. Fini [16], M. Fiorini [18,g], M. Firlej [32], C. Fitzpatrick [45], T. Fiutowski [32], F. Fleuret [9,b], M. Fontana [44], F. Fontanelli [21,h], R. Forty [44], V. Franco Lima [56], M. Frank [44], C. Frei [44], J. Fu [23,q], W. Funk [44], E. Gabriel [54], A. Gallas Torreira [43], D. Galli [17,e], S. Gallorini [25], S. Gambetta [54], Y. Gan [3], M. Gandelman [2], P. Gandini [23], Y. Gao [3], L.M. Garcia Martin [76], J. García Pardiñas [46], B. Garcia Plana [43], J. Garra Tico [51], L. Garrido [42], D. Gascon [42], C. Gaspar [44], G. Gazzoni [7], D. Gerick [14], E. Gersabeck [58], M. Gersabeck [58], T. Gershon [52], D. Gerstel [8], Ph. Ghez [6], V. Gibson [51], O.G. Girard [45], P. Gironella Gironell [42], L. Giubega [34], K. Gizdov [54], V.V. Gligorov [10], C. Göbel [65], D. Golubkov [35], A. Golutvin [57,73], A. Gomes [1,a], I.V. Gorelov [36], C. Gotti [22,i], E. Govorkova [29], J.P. Grabowski [14], R. Graciani Diaz [42], L.A. Granado Cardoso [44], E. Graugés [42], E. Graverini [46], G. Graziani [19], A. Grecu [34], R. Greim [29], P. Griffith [24], L. Grillo [58], L. Gruber [44], B.R. Gruberg Cazon [59], C. Gu [3], E. Gushchin [37], A. Guth [11], Yu. Guz [40,44], T. Gys [44], T. Hadavizadeh [59], C. Hadjivasiliou [7], G. Haefeli [45], C. Haen [44], S.C. Haines [51], B. Hamilton [62], X. Han [14], T.H. Hancock [59], S. Hansmann-Menzemer [14], N. Harnew [59], T. Harrison [56], C. Hasse [44], M. Hatch [44], J. He [4], M. Hecker [57], K. Heinicke [12], A. Heister [12], K. Hennessy [56], L. Henry [76], M. Heß [70], J. Heuel [11], A. Hicheur [64], R. Hidalgo Charman [58], D. Hill [59], M. Hilton [58], P.H. Hopchev [45], J. Hu [14], W. Hu [68], W. Huang [4], Z.C. Huard [61], W. Hulsbergen [29], T. Humair [57], M. Hushchyn [74], D. Hutchcroft [56], D. Hynds [29], P. Ibis [12], M. Idzik [32], P. Ilten [49], A. Inglessi [41], A. Inyakin [40], K. Ivshin [41], R. Jacobsson [44], S. Jakobsen [44], J. Jalocha [59], E. Jans [29], B.K. Jashal [76], A. Jawahery [62], F. Jiang [3], M. John [59], D. Johnson [44], C.R. Jones [51], C. Joram [44], B. Jost [44], N. Jurik [59], S. Kandybei [47], M. Karacson [44], J.M. Kariuki [50], S. Karodia [55], N. Kazeev [74], M. Kecke [14], F. Keizer [51], M. Kelsey [63], M. Kenzie [51], T. Ketel [30], B. Khanji [44], A. Kharisova [75], C. Khurewathanakul [45], K.E. Kim [63], T. Kirn [11], V.S. Kirsebom [45], S. Klaver [20], K. Klimaszewski [33], S. Koliiev [48], M. Kolpin [14], R. Kopecna [14], P. Koppenburg [29], I. Kostiuk [29,48],

S. Kotriakhova [41], M. Kozeiha [7], L. Kravchuk [37], M. Kreps [52], F. Kress [57], S. Kretzschmar [11], P. Krokovny [39,x], W. Krupa [32], W. Krzemien [33], W. Kucewicz [31,l], M. Kucharczyk [31], V. Kudryavtsev [39,x], G.J. Kunde [78], A.K. Kuonen [45], T. Kvaratskheliya [35], D. Lacarrere [44], G. Lafferty [58], A. Lai [24], D. Lancierini [46], G. Lanfranchi [20], C. Langenbruch [11], T. Latham [52], C. Lazzeroni [49], R. Le Gac [8], R. Lefèvre [7], A. Leflat [36], F. Lemaitre [44], O. Leroy [8], T. Lesiak [31], B. Leverington [14], H. Li [66], P.-R. Li [4,ab], Y. Li [5], Z. Li [63], X. Liang [63], T. Likhomanenko [72], R. Lindner [44], F. Lionetto [46], V. Lisovskyi [9], G. Liu [66], X. Liu [3,*], D. Loh [52], A. Loi [24], I. Longstaff [55], J.H. Lopes [2], G. Loustau [46], G.H. Lovell [51], D. Lucchesi [25,o], M. Lucio Martinez [43], Y. Luo [3], A. Lupato [25], E. Luppi [18,g], O. Lupton [52], A. Lusiani [26], X. Lyu [4], F. Machefert [9], F. Maciuc [34], V. Macko [45], P. Mackowiak [12], S. Maddrell-Mander [50], O. Maev [41,44], K. Maguire [58], D. Maisuzenko [41], M.W. Majewski [32], S. Malde [59], B. Malecki [44], A. Malinin [72], T. Maltsev [39,x], H. Malygina [14], G. Manca [24,f], G. Mancinelli [8], D. Marangotto [23,q], J. Maratas [7,w], J.F. Marchand [6], U. Marconi [17], C. Marin Benito [9], M. Marinangeli [45], P. Marino [45], J. Marks [14], P.J. Marshall [56], G. Martellotti [28], M. Martinelli [44,22], D. Martinez Santos [43], F. Martinez Vidal [76], A. Massafferri [1], M. Materok [11], R. Matev [44], A. Mathad [46], Z. Mathe [44], V. Matiunin [35], C. Matteuzzi [22], K.R. Mattioli [77], A. Mauri [46], E. Maurice [9,b], B. Maurin [45], M. McCann [57,44], A. McNab [58], R. McNulty [15], J.V. Mead [56], B. Meadows [61], C. Meaux [8], N. Meinert [70], D. Melnychuk [33], M. Merk [29], A. Merli [23,q], E. Michielin [25], D.A. Milanes [69], E. Millard [52], M.-N. Minard [6], L. Minzoni [18,g], D.S. Mitzel [14], A. Mödden [12], A. Mogini [10], R.D. Moise [57], T. Mombächer [12], I.A. Monroy [69], S. Monteil [7], M. Morandin [25], G. Morello [20], M.J. Morello [26,t], J. Moron [32], A.B. Morris [8], R. Mountain [63], F. Muheim [54], M. Mukherjee [68], M. Mulder [29], D. Müller [44], J. Müller [12], K. Müller [46], V. Müller [12], C.H. Murphy [59], D. Murray [58], P. Naik [50], T. Nakada [45], R. Nandakumar [53], A. Nandi [59], T. Nanut [45], I. Nasteva [2], M. Needham [54], N. Neri [23,q], S. Neubert [14], N. Neufeld [44], R. Newcombe [57], T.D. Nguyen [45], C. Nguyen-Mau [45,n], S. Nieswand [11], R. Niet [12], N. Nikitin [36], N.S. Nolte [44], A. Oblakowska-Mucha [32], V. Obraztsov [40], S. Ogilvy [55], D.P. O'Hanlon [17], R. Oldeman [24,f], C.J.G. Onderwater [71], J.D. Osborn [77], A. Ossowska [31], J.M. Otalora Goicochea [2], T. Ovsiannikova [35], P. Owen [46], A. Oyanguren [76], P.R. Pais [45], T. Pajero [26,t], A. Palano [16], M. Palutan [20], G. Panshin [75], A. Papanestis [53], M. Pappagallo [54], L.L. Pappalardo [18,g], W. Parker [62], C. Parkes [58,44], G. Passaleva [19,44], A. Pastore [16], M. Patel [57], C. Patrignani [17,e], A. Pearce [44], A. Pellegrino [29], G. Penso [28], M. Pepe Altarelli [44], S. Perazzini [44], D. Pereima [35], P. Perret [7], L. Pescatore [45], K. Petridis [50], A. Petrolini [21,h], A. Petrov [72], S. Petrucci [54], M. Petruzzo [23,q], B. Pietrzyk [6], G. Pietrzyk [45], M. Pikies [31], M. Pili [59], D. Pinci [28], J. Pinzino [44], F. Pisani [44], A. Piucci [14], V. Placinta [34], S. Playfer [54], J. Plews [49], M. Plo Casasus [43], F. Polci [10], M. Poli Lener [20], M. Poliakova [63], A. Poluektov [8], N. Polukhina [73,c], I. Polyakov [63], E. Polycarpo [2], G.J. Pomery [50], S. Ponce [44], A. Popov [40], D. Popov [49,13], S. Poslavskii [40], E. Price [50], C. Prouve [43], V. Pugatch [48], A. Puig Navarro [46], H. Pullen [59], G. Punzi [26,p], W. Qian [4], J. Qin [4], R. Quagliani [10], B. Quintana [7], N.V. Raab [15], B. Rachwal [32], J.H. Rademacker [50], M. Rama [26], M. Ramos Pernas [43], M.S. Rangel [2], F. Ratnikov [38,74], G. Raven [30], M. Ravonel Salzgeber [44], M. Reboud [6], F. Redi [45], S. Reichert [12], F. Reiss [10], C. Remon Alepuz [76], Z. Ren [3], V. Renaudin [59], S. Ricciardi [53], S. Richards [50], K. Rinnert [56], P. Robbe [9], A. Robert [10], A.B. Rodrigues [45], E. Rodrigues [61], J.A. Rodriguez Lopez [69], M. Roehrken [44], S. Roiser [44], A. Rollings [59], V. Romanovskiy [40], A. Romero Vidal [43], J.D. Roth [77], M. Rotondo [20], M.S. Rudolph [63], T. Ruf [44], J. Ruiz Vidal [76], J.J. Saborido Silva [43], N. Sagidova [41], B. Saitta [24,f], V. Salustino Guimaraes [65], C. Sanchez Gras [29], C. Sanchez Mayordomo [76], B. Sanmartin Sedes [43], R. Santacesaria [28], C. Santamarina Rios [43], M. Santimaria [20,44], E. Santovetti [27,j], G. Sarpis [58], A. Sarti [20,k], C. Satriano [28,s], A. Satta [27], M. Saur [4], D. Savrina [35,36], S. Schael [11], M. Schellenberg [12], M. Schiller [55], H. Schindler [44], M. Schmelling [13], T. Schmelzer [12], B. Schmidt [44], O. Schneider [45], A. Schopper [44], H.F. Schreiner [61], M. Schubiger [45], S. Schulte [45], M.H. Schune [9], R. Schwemmer [44], B. Sciascia [20], A. Sciubba [28,k], A. Semennikov [35], E.S. Sepulveda [10], A. Sergi [49,44], N. Serra [46], J. Serrano [8], L. Sestini [25], A. Seuthe [12], P. Seyfert [44], M. Shapkin [40], T. Shears [56], L. Shekhtman [39,x], V. Shevchenko [72], E. Shmanin [73], B.G. Siddi [18], R. Silva Coutinho [46], L. Silva de Oliveira [2], G. Simi [25,o], S. Simone [16,d], I. Skiba [18], N. Skidmore [14], T. Skwarnicki [63], M.W. Slater [49], J.G. Smeaton [51], E. Smith [11], I.T. Smith [54], M. Smith [57], M. Soares [17], l. Soares Lavra [1], M.D. Sokoloff [61], F.J.P. Soler [55], B. Souza De Paula [2], B. Spaan [12], E. Spadaro Norella [23,q], P. Spradlin [55], F. Stagni [44], M. Stahl [14], S. Stahl [44], P. Stefko [45], S. Stefkova [57], O. Steinkamp [46], S. Stemmle [14], O. Stenyakin [40], M. Stepanova [41], H. Stevens [12], A. Stocchi [9], S. Stone [63], S. Stracka [26], M.E. Stramaglia [45], M. Straticiuc [34], U. Straumann [46], S. Strokov [75], J. Sun [3], L. Sun [67], Y. Sun [62],

K. Swientek [32], A. Szabelski [33], T. Szumlak [32], M. Szymanski [4], Z. Tang [3], T. Tekampe [12], G. Tellarini [18], F. Teubert [44], E. Thomas [44], M.J. Tilley [57], V. Tisserand [7], S. T'Jampens [6], M. Tobin [5], S. Tolk [44], L. Tomassetti [18,g], D. Tonelli [26], D.Y. Tou [10], R. Tourinho Jadallah Aoude [1], E. Tournefier [6], M. Traill [55], M.T. Tran [45], A. Trisovic [51], A. Tsaregorodtsev [8], G. Tuci [26,44,p], A. Tully [51], N. Tuning [29], A. Ukleja [33], A. Usachov [9], A. Ustyuzhanin [38,74], U. Uwer [14], A. Vagner [75], V. Vagnoni [17], A. Valassi [44], S. Valat [44], G. Valenti [17], M. van Beuzekom [29], H. Van Hecke [78], E. van Herwijnen [44], C.B. Van Hulse [15], J. van Tilburg [29], M. van Veghel [29], R. Vazquez Gomez [44], P. Vazquez Regueiro [43], C. Vázquez Sierra [29], S. Vecchi [18], J.J. Velthuis [50], M. Veltri [19,r], A. Venkateswaran [63], M. Vernet [7], M. Veronesi [29], M. Vesterinen [52], J.V. Viana Barbosa [44], D. Vieira [4], M. Vieites Diaz [43], H. Viemann [70], X. Vilasis-Cardona [42,m], A. Vitkovskiy [29], M. Vitti [51], V. Volkov [36], A. Vollhardt [46], D. Vom Bruch [10], B. Voneki [44], A. Vorobyev [41], V. Vorobyev [39,x], N. Voropaev [41], R. Waldi [70], J. Walsh [26], J. Wang [5], M. Wang [3], Y. Wang [68], Z. Wang [46], D.R. Ward [51], H.M. Wark [56], N.K. Watson [49], D. Websdale [57], A. Weiden [46], C. Weisser [60], M. Whitehead [11], G. Wilkinson [59], M. Wilkinson [63], I. Williams [51], M. Williams [60], M.R.J. Williams [58], T. Williams [49], F.F. Wilson [53], M. Winn [9], W. Wislicki [33], M. Witek [31], G. Wormser [9], S.A. Wotton [51], K. Wyllie [44], D. Xiao [68], Y. Xie [68], H. Xing [66], A. Xu [3], M. Xu [68], Q. Xu [4], Z. Xu [6], Z. Xu [3], Z. Yang [3], Z. Yang [62], Y. Yao [63], L.E. Yeomans [56], H. Yin [68], J. Yu [68,aa], X. Yuan [63], O. Yushchenko [40], K.A. Zarebski [49], M. Zavertyaev [13,c], M. Zeng [3], D. Zhang [68], L. Zhang [3], W.C. Zhang [3,z], Y. Zhang [44], A. Zhelezov [14], Y. Zheng [4], X. Zhu [3], V. Zhukov [11,36], J.B. Zonneveld [54], S. Zucchelli [17,e]

[1] *Centro Brasileiro de Pesquisas Físicas (CBPF), Rio de Janeiro, Brazil*
[2] *Universidade Federal do Rio de Janeiro (UFRJ), Rio de Janeiro, Brazil*
[3] *Center for High Energy Physics, Tsinghua University, Beijing, China*
[4] *University of Chinese Academy of Sciences, Beijing, China*
[5] *Institute of High Energy Physics (ihep), Beijing, China*
[6] *Univ. Grenoble Alpes, Univ. Savoie Mont Blanc, CNRS, IN2P3-LAPP, Annecy, France*
[7] *Université Clermont Auvergne, CNRS/IN2P3, LPC, Clermont-Ferrand, France*
[8] *Aix Marseille Univ, CNRS/IN2P3, CPPM, Marseille, France*
[9] *LAL, Univ. Paris-Sud, CNRS/IN2P3, Université Paris-Saclay, Orsay, France*
[10] *LPNHE, Sorbonne Université, Paris Diderot Sorbonne Paris Cité, CNRS/IN2P3, Paris, France*
[11] *I. Physikalisches Institut, RWTH Aachen University, Aachen, Germany*
[12] *Fakultät Physik, Technische Universität Dortmund, Dortmund, Germany*
[13] *Max-Planck-Institut für Kernphysik (MPIK), Heidelberg, Germany*
[14] *Physikalisches Institut, Ruprecht-Karls-Universität Heidelberg, Heidelberg, Germany*
[15] *School of Physics, University College Dublin, Dublin, Ireland*
[16] *INFN Sezione di Bari, Bari, Italy*
[17] *INFN Sezione di Bologna, Bologna, Italy*
[18] *INFN Sezione di Ferrara, Ferrara, Italy*
[19] *INFN Sezione di Firenze, Firenze, Italy*
[20] *INFN Laboratori Nazionali di Frascati, Frascati, Italy*
[21] *INFN Sezione di Genova, Genova, Italy*
[22] *INFN Sezione di Milano-Bicocca, Milano, Italy*
[23] *INFN Sezione di Milano, Milano, Italy*
[24] *INFN Sezione di Cagliari, Monserrato, Italy*
[25] *INFN Sezione di Padova, Padova, Italy*
[26] *INFN Sezione di Pisa, Pisa, Italy*
[27] *INFN Sezione di Roma Tor Vergata, Roma, Italy*
[28] *INFN Sezione di Roma La Sapienza, Roma, Italy*
[29] *Nikhef National Institute for Subatomic Physics, Amsterdam, Netherlands*
[30] *Nikhef National Institute for Subatomic Physics and VU University Amsterdam, Amsterdam, Netherlands*
[31] *Henryk Niewodniczanski Institute of Nuclear Physics Polish Academy of Sciences, Kraków, Poland*
[32] *AGH – University of Science and Technology, Faculty of Physics and Applied Computer Science, Kraków, Poland*
[33] *National Center for Nuclear Research (NCBJ), Warsaw, Poland*
[34] *Horia Hulubei National Institute of Physics and Nuclear Engineering, Bucharest-Magurele, Romania*
[35] *Institute of Theoretical and Experimental Physics NRC Kurchatov Institute (ITEP NRC KI), Moscow, Russia*
[36] *Institute of Nuclear Physics, Moscow State University (SINP MSU), Moscow, Russia*
[37] *Institute for Nuclear Research of the Russian Academy of Sciences (INR RAS), Moscow, Russia*
[38] *Yandex School of Data Analysis, Moscow, Russia*
[39] *Budker Institute of Nuclear Physics (SB RAS), Novosibirsk, Russia*
[40] *Institute for High Energy Physics NRC Kurchatov Institute (IHEP NRC KI), Protvino, Russia*
[41] *Petersburg Nuclear Physics Institute NRC Kurchatov Institute (PNPI NRC KI), Gatchina, Russia, St. Petersburg, Russia*
[42] *ICCUB, Universitat de Barcelona, Barcelona, Spain*
[43] *Instituto Galego de Física de Altas Enerxías (IGFAE), Universidade de Santiago de Compostela, Santiago de Compostela, Spain*
[44] *European Organization for Nuclear Research (CERN), Geneva, Switzerland*
[45] *Institute of Physics, Ecole Polytechnique Fédérale de Lausanne (EPFL), Lausanne, Switzerland*
[46] *Physik-Institut, Universität Zürich, Zürich, Switzerland*
[47] *NSC Kharkiv Institute of Physics and Technology (NSC KIPT), Kharkiv, Ukraine*
[48] *Institute for Nuclear Research of the National Academy of Sciences (KINR), Kyiv, Ukraine*
[49] *University of Birmingham, Birmingham, United Kingdom*
[50] *H.H. Wills Physics Laboratory, University of Bristol, Bristol, United Kingdom*
[51] *Cavendish Laboratory, University of Cambridge, Cambridge, United Kingdom*

[52] Department of Physics, University of Warwick, Coventry, United Kingdom
[53] STFC Rutherford Appleton Laboratory, Didcot, United Kingdom
[54] School of Physics and Astronomy, University of Edinburgh, Edinburgh, United Kingdom
[55] School of Physics and Astronomy, University of Glasgow, Glasgow, United Kingdom
[56] Oliver Lodge Laboratory, University of Liverpool, Liverpool, United Kingdom
[57] Imperial College London, London, United Kingdom
[58] School of Physics and Astronomy, University of Manchester, Manchester, United Kingdom
[59] Department of Physics, University of Oxford, Oxford, United Kingdom
[60] Massachusetts Institute of Technology, Cambridge, MA, United States
[61] University of Cincinnati, Cincinnati, OH, United States
[62] University of Maryland, College Park, MD, United States
[63] Syracuse University, Syracuse, NY, United States
[64] Laboratory of Mathematical and Subatomic Physics, Constantine, Algeria, associated to [2]
[65] Pontifícia Universidade Católica do Rio de Janeiro (PUC-Rio), Rio de Janeiro, Brazil, associated to [2]
[66] South China Normal University, Guangzhou, China, associated to [3]
[67] School of Physics and Technology, Wuhan University, Wuhan, China, associated to [3]
[68] Institute of Particle Physics, Central China Normal University, Wuhan, Hubei, China, associated to [3]
[69] Departamento de Fisica, Universidad Nacional de Colombia, Bogota, Colombia, associated to [10]
[70] Institut für Physik, Universität Rostock, Rostock, Germany, associated to [14]
[71] Van Swinderen Institute, University of Groningen, Groningen, Netherlands, associated to [29]
[72] National Research Centre Kurchatov Institute, Moscow, Russia, associated to [35]
[73] National University of Science and Technology "MISIS", Moscow, Russia, associated to [35]
[74] National Research University Higher School of Economics, Moscow, Russia, associated to [38]
[75] National Research Tomsk Polytechnic University, Tomsk, Russia, associated to [35]
[76] Instituto de Fisica Corpuscular, Centro Mixto Universidad de Valencia - CSIC, Valencia, Spain, associated to [42]
[77] University of Michigan, Ann Arbor, United States, associated to [63]
[78] Los Alamos National Laboratory (LANL), Los Alamos, United States, associated to [63]

* Corresponding author.
E-mail address: xuesong.liu@cern.ch (X. Liu).
[a] Universidade Federal do Triângulo Mineiro (UFTM), Uberaba-MG, Brazil.
[b] Laboratoire Leprince-Ringuet, Palaiseau, France.
[c] P.N. Lebedev Physical Institute, Russian Academy of Science (LPI RAS), Moscow, Russia.
[d] Università di Bari, Bari, Italy.
[e] Università di Bologna, Bologna, Italy.
[f] Università di Cagliari, Cagliari, Italy.
[g] Università di Ferrara, Ferrara, Italy.
[h] Università di Genova, Genova, Italy.
[i] Università di Milano Bicocca, Milano, Italy.
[j] Università di Roma Tor Vergata, Roma, Italy.
[k] Università di Roma La Sapienza, Roma, Italy.
[l] AGH - University of Science and Technology, Faculty of Computer Science, Electronics and Telecommunications, Kraków, Poland.
[m] LIFAELS, La Salle, Universitat Ramon Llull, Barcelona, Spain.
[n] Hanoi University of Science, Hanoi, Vietnam.
[o] Università di Padova, Padova, Italy.
[p] Università di Pisa, Pisa, Italy.
[q] Università degli Studi di Milano, Milano, Italy.
[r] Università di Urbino, Urbino, Italy.
[s] Università della Basilicata, Potenza, Italy.
[t] Scuola Normale Superiore, Pisa, Italy.
[u] Università di Modena e Reggio Emilia, Modena, Italy.
[v] H.H. Wills Physics Laboratory, University of Bristol, Bristol, United Kingdom.
[w] MSU – Iligan Institute of Technology (MSU-IIT), Iligan, Philippines.
[x] Novosibirsk State University, Novosibirsk, Russia.
[y] Sezione INFN di Trieste, Trieste, Italy.
[z] School of Physics and Information Technology, Shaanxi Normal University (SNNU), Xi'an, China.
[aa] Physics and Micro Electronic College, Hunan University, Changsha City, China.
[ab] Lanzhou University, Lanzhou, China.
[†] Deceased.